cm^{-1}). In view of the complexity of the system, the inherent experimental difficulties, and the differences in ionic strengths, we regard the spectrophotometric values of the successive formation constants as being in satisfactory agreement.

All three spectra shown in Figure 5 clearly belong to species with more or less octahedral coordination. All three spin-allowed bands are present, and the shoulder on the high-energy side of the middle band is plausibly assigned to the $^3A_2 \rightarrow {}^1E$ transition intensified by singlet–triplet mixing. It will be seen from Figure 5 that the spectrum of nickel(II) in the molten $LiNO_3$–$NaNO_3$–KNO_3 eutectic at 125° is strikingly similar to that of the $Ni(NO_3)_3^-$ complex in molten dimethyl sulfone at the same temperature. Thus we suppose that the same entities are present in both media. Since nickel(II) can only be complexed to NO_3^- in the nitrate melt, we conclude that nitrate behaves as a bidentate ligand in a distorted octahedral structure. Also, we suppose that the two nitrate ions in the dinitrato complex may act either as bidentate ligands and occupy planar positions or as unidentate ligands and occupy pyramidal positions. (Attempts are being made to prepare the dinitrato and trinitrato complexes in solid form for X-ray structure determinations.)

Although the coordination of nickel(II) in the $LiNO_3$–$NaNO_3$–KNO_3 eutectic at 125° appears to have a well-defined geometry, it is by no means certain that such regularity persists up to significantly higher temperatures. A progressive broadening of the distribution of coordination geometries with increasing temperature, such as occurs in chloride systems,[9] almost certainly will also occur in molten nitrates. The only question is whether or not this broadening becomes significant at temperatures below those at which the melt decomposes.

The compound methyltriphenylarsonium tetranitratonickelate(II) has been reported in the literature.[10] Although the data presented here do not eliminate entirely the possibility that the entity in the melt is the 1:4 complex, a published spectrum,[10] presumed to be that of the 1:4 complex, is substantially different from the melt spectrum presented here.

[9] J. Brynestad, C. R. Boston, and G. P. Smith, *J. Chem. Phys.*, **47**, 3179 (1967); and J. Brynestad and G. P. Smith, *ibid.*, **47**, 3190 (1967).

[10] D. K. Straub, R. S. Drago, and J. T. Donoghue, *Inorg. Chem.*, **1**, 848 (1962).

CONTRIBUTION FROM THE RESEARCH AND DEVELOPMENT LABORATORIES
OF THE CORNING GLASS WORKS, CORNING, NEW YORK 14830

Reactions between Sodium Carboxylic Acid Salts and Molten Sodium Nitrate and Sodium Nitrite

BY T. R. KOZLOWSKI AND R. F. BARTHOLOMEW

Received May 16, 1968

The over-all reactions of NaCOOH and $NaC_2H_3O_2$ in $NaNO_3$ and $NaNO_2$ have been examined using infrared analysis, cryoscopy, voltammetry, and chronopotentiometry. The over-all reactions with NaCOOH are

$$NaCOOH + NaNO_3 \longrightarrow NaNO_2 + {}^1/_2Na_2CO_3 + {}^1/_2H_2O + {}^1/_2CO_2$$

and

$$NaCOOH + NaNO_2 \longrightarrow Na_2CO_3 + {}^1/_2N_2O + {}^1/_2H_2O$$

Similarly with $NaC_2H_3O_2$ the reactions are

$$NaC_2H_3O_2 + 4NaNO_3 \longrightarrow {}^1/_2Na_2CO_3 + {}^3/_2H_2O + 4NaNO_2$$

and

$$NaC_2H_3O_2 + 3NaNO_2 \longrightarrow 2Na_2CO_3 + {}^3/_2H_2O + {}^1/_2N_2O + N_2$$

The reactions with NaCOOH were much more rapid than the reactions with $NaC_2H_3O_2$ in $NaNO_3$ at approximately 320°. The need for caution in examining these systems is stressed because of the danger of explosions at high concentrations of carboxylic acid salts. Equations are proposed for the reaction of $NaC_3H_5O_2$ with $NaNO_3$ by generalizing from the reaction schemes given for formate and acetate. The predicted values for the number of cryoscopic species generated in $NaNO_3$ agreed well with those experimentally found in the same system.

Introduction

Reactions between molten salts and organic materials have been of interest because of the potential of such systems for producing useful organic and metalloorganic compounds. Sundermeyer[1] has reviewed such systems. More recent work has also considered the use of molten nitrates for synthesizing nitrobenzenes.[2] Studies of simpler species, such as carboxylic acid salts in inorganic nitrate melts, have also been reported. Thus Guenther[3] demonstrated the ability of sodium

[1] W. Sundermeyer, *Angew. Chem. Intern. Ed. Engl.*, **4**, 222 (1965).

[2] R. B. Temple, C. Fay, and J. Williamson, *Chem. Commun.*, 966 (1967).

[3] K. F. Guenther, *J. Phys. Chem.*, **67**, 2851 (1963).

acetate and propionate to lower the surface tension of a $LiNO_3$–KNO_3 eutectic melt. Sokolov[4,5] has reported the phase diagrams of sodium salts of fatty acids in sodium nitrate and nitrite. These systems were reported to have a tendency to explode at higher concentrations of the organic constituent. Shams El Din and El Hosary[6] looked at the reactions of sodium oxalate, formate, and acetate in acid–base titrations of KPO_3 and $K_2Cr_2O_7$ in molten KNO_3. The extent to which a quantitative description of the reaction of the "organic" salt in the nitrate melt was provided was meager. Only the formation of nitrite and carbonate had been definitely established.

It is the purpose of this work to examine the reactions of carboxylic acid salts in molten sodium nitrate in greater detail. Extension of the study to include sodium nitrite followed naturally from the initial experimental results. Emphasis has been placed on the determination of the reaction products, and the determination of the over-all stoichiometry of the reactions of sodium formate and acetate in sodium nitrate and nitrite.

Experimental Section

Chemicals.—The following "Baker Analyzed" reagent grade chemicals were used: $NaNO_3$, $NaNO_2$, $NaCOOH$, and $NaC_2H_3O_2\cdot 3H_2O$. The Fisher Scientific Co. supplied an NF grade of $NaC_3H_5O_2$. The sodium acetate trihydrate and sodium nitrite were vacuum dried, while the other chemicals were dried in air at 130°. All chemicals were used directly without additional purification. Spectroscopic grade KBr, obtained from the Harshaw Chemical Co., was used in the infrared studies.

Cryoscopy.—The cryoscopic technique and basic apparatus have been previously described.[7,8] The data were analyzed according to

$$\frac{\Delta T}{K_f m} = \nu \qquad (1)$$

where ΔT is the temperature lowering of the solvent melting point, in degrees Kelvin, caused by the addition of acetate or formate of molality m. The number of distinguishable species generated in the melt is given by ν, and K_f, the molal cryoscopic constant, is given by

$$\frac{RT_0^2}{\Delta H_f n} = K_f \qquad (2)$$

The solvent melting point T_0 was taken as 579.96°K, and the heat of fusion ΔH_f was taken as 3520 cal/mol.[9] This provides a value of 16.14°/mol for the molal cryoscopic constant of $NaNO_3$.

Infrared Spectra.—All spectra were obtained on a Beckman IR-12 infrared spectrophotometer. Solid samples were examined by the conventional KBr-pressed-disk techniques. Gaseous samples were examined in a 10-cm gas cell with NaCl windows. With the solid samples, assignment of frequencies to particular anions was based on comparison of the sample spectra with similarly made "control" disks of $NaNO_3$, $NaNO_2$, Na_2CO_3, $NaC_2H_3O_2$, or $NaCOOH$, as well as specially prepared mixtures of Na_2CO_3 in $NaNO_3$ and $NaNO_2$, and $NaNO_2$ in $NaNO_3$. All observed frequencies agreed well with values reported by Nakamoto.[10]

The following procedure was used to obtain spectra of the reaction products. Approximately 20 wt % of $NaCOOH$ or $NaC_2H_3O_2$ was added to molten $NaNO_3$ (350°) and $NaNO_2$ (325°). The mixtures were held at temperature until the bubbling subsided, then quenched, ground while still hot, sieved, mixed with KBr, and pressed into disks.

To obtain spectra of the gaseous reaction products, a reaction cell containing 50 g of $NaNO_3$ or $NaNO_2$ (330°) was connected to the gas cell already mounted in the spectrometer. Dried, decarbonated argon was passed over the melt to establish a background spectrum. $NaCOOH$ or $NaC_2H_3O_2$ (1–2 wt %) was dropped into the melt without breaking the purge. The gaseous or volatile reaction products were swept up into the gas cell by the flowing argon, and the spectra were recorded. The temperature was continuously monitored and did increase about 2° during the course of each experiment.

Voltammetry and Chronopotentiometry.—Both of these examinations were performed at 320 ± 2° in $NaNO_3$. A Sargent Model XV polarograph, adapted for a three-electrode system, was used to obtain current–voltage curves. A sweep rate of 0.2 V/min was used throughout. The reference electrode was a solution of $AgNO_3$ in $NaNO_3$ (0.06 m Ag^+) contained in a Corning Code 7740 borosilicate glass bulb. The working electrode was a platinum foil, 1-cm square. The indicator electrode was a platinum wire, sealed in a Corning Code 0120 lead silicate glass tube, which was ground flat until the wire was exposed. The electrode area was approximately 3×10^{-3} cm², and the electrode was rotated at 600 rpm during the measurements.

The chronopotentiometry was performed in 300 g of $NaNO_3$ contained in a 400-ml lipless beaker. A pressed asbestos top covered the beaker, with access to the melt provided by holes suitable for three electrodes, a chromel–alumel thermocouple, and a sample addition port. The working and reference electrodes were the same as described above. The indicator was all platinum, consisting of a foil 3 × 3 mm, welded to a length of wire. This was sealed in a Corning Code 0120 glass tube so that only the foil was in contact with the melt. A conventional circuit was used, except that a bias potential of 0.4 V was placed on the anode as described by Inman and Braunstein.[11] The potential–time curves were recorded on a Type 564 Tektronix oscilloscope fitted with an image storing screen. The resulting traces were stored on the screen and photographed on Polaroid 107 film with a Tektronix Model C-12 camera. The chronopotentiometric data were analyzed with the Sand equation

$$i\tau^{1/2} = \frac{\pi^{1/2} nACD^{1/2}}{2} \qquad (3)$$

where the terms have their usual meanings.

Results

Visual Observations.—When $NaC_2H_3O_2$ and $NaCOOH$ are added to molten $NaNO_3$ and $NaNO_2$, the ensuing reactions are vigorous, producing large amounts of colorless gases, and changing the nitrate melt from water white to pale yellow. The danger of explosion is real. For example, five of ten samples containing 30 wt % of $NaC_2H_3O_2$ in $NaNO_3$ exploded without warning after 1 hr at 350°. This did not occur when the amount of acetate was reduced to 10 wt %. Generally, the lower the concentration of carboxylic acid salt, *i.e.*, the more dilute the solution, the higher the allowable operating temperature of the solvent. For example, 3 wt % of $NaC_2H_3O_2$ in $NaNO_3$ at 450° reacted vigorously but produced no explosion.

Cryoscopy.—The results for $NaCOOH$, $NaC_2H_3O_2$,

---

(4) N. M. Sokolov, *Zh. Obshch. Khim.*, **24**, 1150 (1954).

(5) N. M. Sokolov, *ibid.*, **27**, 840 (1957).

(6) A. M. Shams El Din and A. A. El Hosary, *Electrochim. Acta*, **13**, 135 (1968).

(7) G. J. Janz and C. Solomons, *Rev. Sci. Instr.*, **29**, 302 (1958).

(8) G. J. Janz and C. Solomons, *Anal. Chem.*, **31**, 623 (1959).

(9) G. J. Janz and T. R. Kozlowski, *J. Phys. Chem.*, **67**, 2857 (1963).

(10) K. Nakamoto, "Infrared Spectra of Inorganic and Coordination Compounds," John Wiley & Sons, Inc., New York, N. Y., 1963, Part II.

(11) D. Inman and J. Braunstein, *Chem. Commun.*, 148 (1966).

and $NaC_3H_5O_2$ as solutes in $NaNO_3$ are shown in Figure 1 in terms of the moles of cryoscopic particles formed, ν, as a function of solute concentration, m. The molalities, temperature changes, and average values of ν are given in Table I. In general, the moles of particles generated by the solutes tend to decrease and level off with concentration. With $NaC_3H_5O_2$, this decrease is more pronounced than with NaCOOH. Ideally, each acid salt should have exhibited a simple freezing point depression caused by the anion; however, this was not the case. The ranges for the formate were from 1.4 for initial additions to 1.0, for the acetate from 3.2 to 2.2, and for the propionate from 3.9 to 2.6 particles/mol of added solute. This drastic departure from ideality, even within the limits of the average deviations shown in Figure 1, gave the initial indication of the complex reactions in these systems.

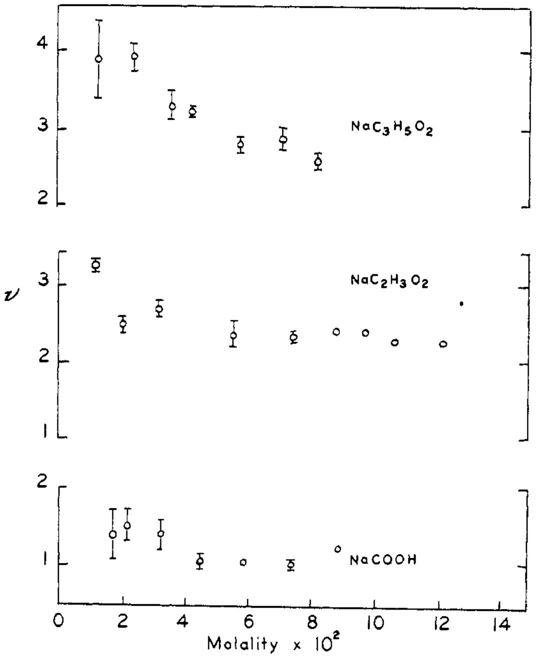

Figure 1.—Values of ν (eq 1) as functions of concentration of NaCOOH, $NaC_2H_3O_2$, and $NaC_3H_5O_2$ in molten $NaNO_3$.

TABLE I

CRYOSCOPIC RESULTS IN $NaNO_3$

10^2m	ΔT, °K	Av ν
NaCOOH solute		
1.637	0.36	1.36
2.267	0.55	1.50
3.218	0.72	1.39
4.495	0.75	1.03
5.827	0.96	1.02
7.431	1.17	0.97
8.874	1.76	1.23
$NaC_2H_3O_2$ solute		
1.091	0.57	3.24
1.091	0.79	3.48
3.132	1.37	2.71
5.454	2.36	2.68
6.504	2.61	2.48
7.792	2.95	2.34
8.669	3.38	2.42
9.609	3.72	2.40
10.600	3.86	2.26
12.138	4.41	2.25
$NaC_3H_5O_2$ solute		
1.177	0.74	3.90
2.275	1.45	3.94
3.469	1.85	3.30
4.647	2.43	3.24
5.727	2.59	2.80
7.065	3.24	2.84
8.058	3.39	2.60
$NaNO_2$ solute		
1.996	0.23	0.71
4.573	0.51	0.69
7.447	0.76	0.63
9.831	1.08	0.68
12.303	1.29	0.65
14.910	1.59	0.66

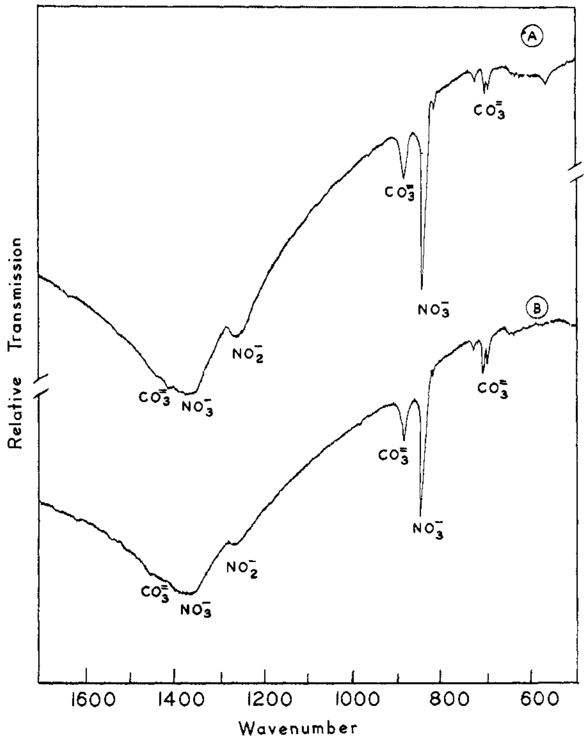

Figure 2.—(A) Spectrum of the quenched melt: NaCOOH + $NaNO_3$. (B) Spectrum of the quenched melt: $NaC_2H_3O_2$ + $NaNO_3$.

Infrared.—Spectra of the quenched samples were examined from 200 to 4000 cm^{-1}, but only the regions of interest are shown in Figures 2–5. Although the concentration levels of NaCOOH and $NaC_2H_3O_2$ initially placed in these samples were much higher than the concentration levels examined in the cryoscopic and polarographic work, it is assumed that the final products of the reactions are the same.

Results of the reaction of NaCOOH and $NaC_2H_3O_2$ in $NaNO_3$ indicated that $NaNO_2$ (830, 1260, and 1328 cm^{-1}) and Na_2CO_3 (695, 702, 880, and 1440 cm^{-1}) were formed in the melt. These spectra are shown in Figure 2. The same systems also produced N_2O (2230 and 1275 cm^{-1}), CO_2 (2350 cm^{-1}), and H_2O (1350 to 1850 cm^{-1}) as gaseous species, as shown in Figure 3. The relative intensity of the CO_2 band is greater with the formate than the acetate because of the faster reaction of formate in $NaNO_3$. The intensity of this same band did increase with time in the $NaC_2H_3O_2$–$NaNO_3$ system.

With $NaNO_2$ as the solvent, addition of NaCOOH and $NaC_2H_3O_2$ produced only Na_2CO_3 in the melt, as shown in Figure 4. Bands at 1360 and 1600 cm^{-1} in Figure 4A are attributable to unreacted formate. The only detectable gases were N_2O and H_2O, as shown in Figure 5, the absence of CO_2 being especially noteworthy. The intensity of the H_2O bands is weak, but some condensation did occur between the reactor and the gas cell. Also the high dilution of water vapor in the dry argon stream caused a reduction in intensity. Nevertheless, qualitative identification of all of these products was positive.

Gases such as H_2, O_2, and N_2 could not be detected

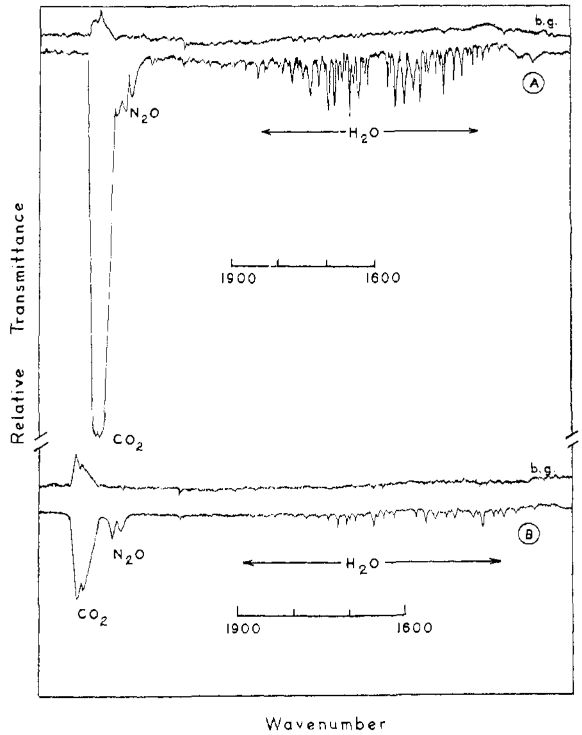

Figure 3.—(A) Spectrum of the gases formed in the reaction: NaCOOH + $NaNO_3$. (B) Spectrum of the gases formed in the reaction: $NaC_2H_3O_2$ + $NaNO_3$.

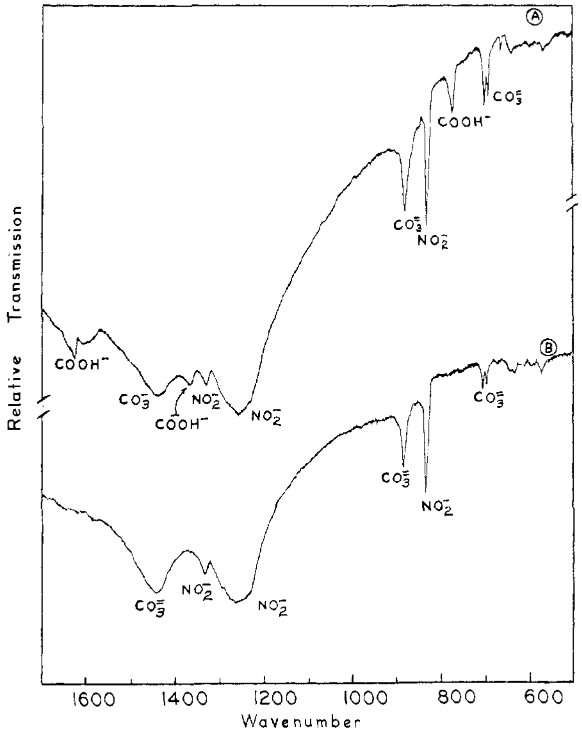

Figure 4.—(A) Spectrum of the quenched melt: 20 wt % NaCOOH + $NaNO_2$. (B) Spectrum of the quenched melt: 20 wt % $NaC_2H_3O_2$ + $NaNO_2$.

using this technique. The presence of sodium oxide would also be difficult to detect in the infrared region. In addition, frequencies characteristic of the hydroxyl ion were not detected in any of the samples.

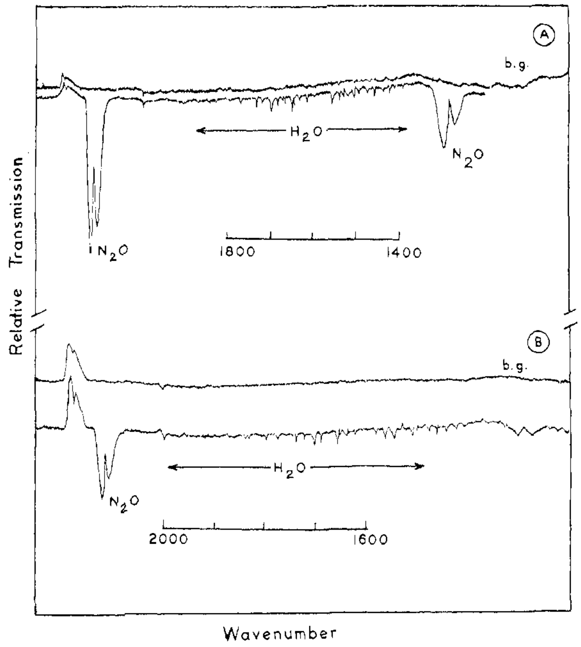

Figure 5.—(A) Spectrum of the gases formed in the reaction: NaCOOH + $NaNO_2$. (B) Spectrum of the gases formed in the reaction: $NaC_2H_3O_2$ + $NaNO_2$.

Voltammetry.—The indicator electrode was calibrated with $NaNO_2$ additions and gave a linear response between limiting current and nitrite concentration up to 5×10^{-3} *m*. The half-wave potential $E_{1/2}$ was 0.56 ± 0.02 V with respect to the Ag–Ag^+ reference electrode. The anodic current–voltage curves obtained from NaCOOH additions to $NaNO_3$ (320 ± 2°) are given in Figure 6. Of the two waves shown, the first occurs with an $E_{1/2}$ of 0.37 ± 0.02 V and the second at an $E_{1/2}$ of 0.56 ± 0.02 V. The second wave is ascribed to nitrite in the melt and serves to confirm the infrared results. Analysis of the first wave was made by plotting log $[(i_d - i)i^{-1}]$ *vs.* *E*, where i_d is the limiting current. The resulting slopes were indicative of a two-electron process. This, coupled with the infrared results and with the similar work of Topol, *et al.*,[12] resulted in assigning the first wave to the formation of carbonate in the melt. An ill-defined third wave was also noted during the initial stages of reaction in this

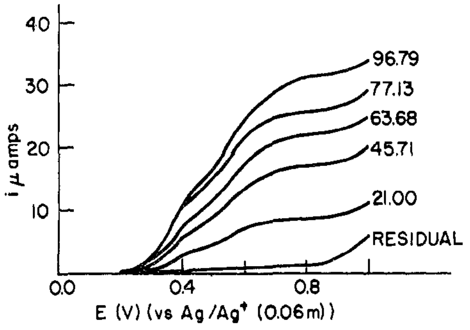

Figure 6.—Anodic voltammetry of sodium formate in sodium nitrate at 322°. (Numbers on curves represent weight of NaCOOH in milligrams added to 500 g of $NaNO_3$.)

---

[12] L. E. Topol, R. A. Osteryoung, and J. H. Christie, *J. Phys. Chem.*, **70**, 2857 (1966).

system. The $E_{1/2}$ was approximately -0.25 ± 0.1 V for this wave. It could not be detected 10 min after the addition of NaCOOH to the melt. We ascribe this wave to the formation of NaOH in the melt, in reasonable agreement with the value of -0.3 V found by Topol, *et al.*,[12] for NaOH in $NaNO_3$–KNO_3 at 300°. Table II summarizes the values of the limiting current due to carbonate and nitrite formation in the melt as a function of added formate. The ratio of moles of nitrite formed to moles of formate added was found to be 0.68 ± 0.04.

TABLE II

VOLTAMMETRY IN $NaNO_3$ (322°)

Solute added, m*M*	Current from CO_3^{2-}, μA	Current from NO_2^-, μA	$[NO_2^-]$, m*M*	$[NO_2^-]$/[COOH]
NaCOOH				
0.309	3.4	4.1	0.214	0.693
0.672	7.1	9.4	0.490	0.729
0.936	9.6	12.1	0.630	0.673
1.134	11.7	14.5	0.755	0.666
1.423	13.8	18.0	0.938	0.659
				Elapsed time, min
$NaC_2H_3O_2$				
0.2990	...	1.05	0.05	10
	...	4.58	0.234	40
	...	7.25	0.378	72
	1.0	9.15	0.477	118
	1.15	11.00	0.573	155
	1.5	11.70	0.610	184
	1.55	12.60	0.656	213
	2.50	14.70	0.766	1165

Addition of $NaC_2H_3O_2$ to $NaNO_3$ gave current–voltage data similar to that found in the reaction with NaCOOH. These data are also summarized in Table II. The ratio of moles of nitrite formed to moles of acetate added was found to be 2.3 ± 0.2.

Chronopotentiometry.—The system was calibrated at 320 ± 2° by using known concentrations of nitrate–nitrite solutions. For currents between 0.82 and 2.15 mA (or for transition times τ between 3.67 and 0.275 sec), eq 3 was obeyed to within 3%. The value of $i\tau^{1/2}/C$ was found to be $(54.5 \pm 1.9) \times 10^{-3}$ mA sec$^{1/2}$ (mol l^{-1})$^{-1}$. The quarter-wave potential $E_{1/4}$ was found to be 0.52 ± 0.02 V for the anodic oxidation of nitrite and is within experimental error of the corresponding half-wave potential obtained from voltammetry. Values of $i\tau^{1/2}$, as functions of time after additions of NaCOOH, are given in Table III. Elimination of the bias of $+0.4$ V on the anode resulted in two waves being formed, indicative of the formation of carbonate from the reaction. A value of $i\tau^{1/2}$ of 0.624 was used as the equivalent to find equilibrium conditions. This corresponds to a ratio of 1.2 mol of nitrite formed for each mole of formate added.

The reactions between $NaC_2H_3O_2$ and $NaNO_3$, examined in a similar manner, are summarized in Table III. The final equilibrium value for $i\tau^{1/2}$ was taken as 1.07 after 24 hr. This value remained constant even beyond this arbitrary cutoff time. This corresponds to 1.9 mol of nitrite formed for each mole of acetate added to the melt.

TABLE III

CHRONOPOTENTIOMETRY IN $NaNO_3$ (319 ± 1°)

Time after additions	τ, sec	$i\tau^{1/2}$, mA sec$^{1/2}$	Av $i\tau^{1/2}$, mA sec$^{1/2}$
9.640×10^{-3} *M* NaCOOH Solute, $i = 1.035$ mA			
4 min	0.255	0.491	
9 min	0.3167	0.583	
10 min	0.2900	0.557	
15 min	0.2900	0.557	
16 min	0.2667	0.535	
20 min	0.3556	0.618	
21 min	0.3667	0.627	
30 min	0.3600	0.621	
31 min	0.3700	0.630	
60 min	0.360	0.621	
80 min	0.370	0.630	0.624 ± 0.006
120 min	0.360	0.621	
10.373×10^{-3} *M* $Na_2C_2H_3O_2$ Solute, $i = 1.01$ mA			
24 hr	1.133	1.075	
	1.028	1.024	
27 hr	1.089	1.054	
31.5 hr	1.200	1.106	1.07 ± 0.03

A comparison of the cryoscopic and electrochemical results for reaction in $NaNO_3$ is summarized in Table IV.

TABLE IV

CRYOSCOPIC, VOLTAMMETRIC, AND CHRONOPOTENTIOMETRIC RESULTS WITH NaCOOH AND $NaC_2H_3O_2$ IN $NaNO_3$

Solute	Method	Wave potentials, V	Products	$[NO_2^-]$/[solute]	ν(calcd)	ν(obsd)
NaCOOH	*a*	$E_{1/2} = -0.25$	NaOH			
		$E_{1/2} = 0.37$	Na_2CO_3			
		$E_{1/2} = 0.56$	$NaNO_2$	0.68	1.06	
	b	$E_{1/4} = 0.52$	$NaNO_2$	1.2	1.3	
	c		$NaNO_2$, Na_2CO_3		1.2–0.75	1.2–1.0
$NaC_2H_3O_2$	*a*	$E_{1/2} = 0.36$	Na_2CO_3			
		$E_{1/2} = 0.56$	$NaNO_2$	2.3	2.5	
	b	$E_{1/4} = 0.52$	$NaNO_2$	1.9	2.3	
	c		$NaNO_2$, Na_2CO_3		3.3–1.6	2.3–2.2
$NaC_3H_5O_2$	*c*		$NaNO_2$, Na_2CO_3		5.3–2.4	2.6–2.5

[a] Voltammetry. [b] Chronopotentiometry. [c] Cryoscopy.

Discussion

Any reaction schemes postulated for the reaction of NaCOOH and $NaC_2H_3O_2$ in $NaNO_3$ and $NaNO_2$ must fulfill the requirements imposed by the infrared analysis and the mole ratios of nitrite to carboxylic acid salt obtained from chronopotentiometry and voltammetry, and account for the large values of ν found during the cryoscopic work. It will be most convenient to begin with the reaction of NaCOOH in $NaNO_3$ and $NaNO_2$.

NaCOOH in $NaNO_3$ and $NaNO_2$.—The infrared data postulate the formation of Na_2CO_3, $NaNO_2$, N_2O, H_2O, and CO_2 in $NaNO_3$, but only N_2O, H_2O, and Na_2CO_3 in $NaNO_2$. The relatively low level of N_2O found in the gases examined in the formate–nitrate system (compared to the amount of CO_2, see Figure 3) strongly suggests that two reactions are occurring in the melt. The first is given by

$$NaCOOH + NaNO_3 \longrightarrow NaNO_2 + {}^1/_2Na_2CO_3 + {}^1/_2H_2O + {}^1/_2CO_2 \quad (4)$$

The second involves the reaction of NaCOOH with nitrite formed in the melt and is given by

$$NaCOOH + NaNO_2 \longrightarrow Na_2CO_3 + {}^1/_2N_2O + {}^1/_2H_2O \quad (5)$$

Equations 4 and 5 represent the over-all reactions of sodium formate in $NaNO_3$ and $NaNO_2$, but it becomes necessary to check the quantitative validity of the proposed stoichiometry.

If reaction 4 were the only one occurring and if the amount of solvent, *i.e.*, $NaNO_3$, which is consumed during the reaction is assumed to be negligible in altering the molality of the added formate, then for each mole of formate added, 1 mol of $NaNO_2$ and 0.5 mol of Na_2CO_3 would be detected cryoscopically. The cryoscopic detection of gases is possible,[13] but the concentrations rapidly reach saturation and will contribute significantly only at low concentration levels, *i.e.*, near 1.0×10^{-3} *m*. Then, each mole of $NaNO_2$, because of the formation of solid solutions with $NaNO_3$, contributes 0.7 mol to the lowering of the freezing point. The value of 0.7 was obtained from the $NaNO_2$–$NaNO_3$ phase diagram[14] and verified from independent cryoscopic measurements (Table I). Thus 1 mol of NaCOOH will produce 1.2 particles (0.7 from the $NaNO_2$ and 0.5 from the Na_2CO_3) determined cryoscopically according to eq 4. If the reaction given by eq 5 begins to compete for NaCOOH, the amount of $NaNO_2$ present in the melt decreases, and the amount of carbonate increases. This would tend to lower the over-all moles of cryoscopic particles toward a theoretical limit (summation of eq 4 and 5) of 0.75 particle/mol of formate added. The results for NaCOOH in Figure 1 show that the system levels off at 1.2–1.0 particles, in essential agreement with the stoichiometry of reaction 4, but not totally rejecting a contribution from reaction 5.

The chronopotentiometric results indicate that the ratio of nitrite to formate should be 1.2 ± 0.1. The voltammetric results indicate that the same ratio should be 0.68 ± 0.04. Reaction 4 predicts the ratio to be 1.0, while addition of reactions 4 and 5 would drive the ratio to zero. Since there is nitrite present in the system after completion of the reactions, it is obvious that their relative rates determine the abundance of nitrite in the melt. The apparent discrepancy between the voltammetry and chronopotentiometry may be explained on the grounds that the reaction rates appear to be rapid and are most likely diffusion controlled. Lack of stirring in the chronopotentiometric study would have caused less contact of the nitrite ion with the formate ion in the melt. This predicts that the results of the voltammetry should be in agreement with the cryoscopic data, since the latter system was also extensively stirred. That this is the case is readily shown in the following manner: If x mol from 1 mol of formate partially reacted according to eq 4, then x mol of $NaNO_2$ and $x/2$ mol of Na_2CO_3 would have been formed. If the remainder of the formate, *i.e.*, $1 - x$ mol, completely reacted according to eq 5, then $1 - x$ mol of $NaNO_2$, available only from reaction 4, would also have reacted to produce $1 - x$ mol of Na_2CO_3. The total moles of $NaNO_2$ formed from each mole of NaCOOH becomes $2x - 1$ and must equal the ratio 0.68 ± 0.04. That $x = 0.84$ is readily calculated.

A similar argument based on the chronopotentiometric ratio of 1.2 ± 0.1 leads to the conclusion that $x = 1.1$; *i.e.*, more formate reacted than was actually present. The total moles of cryoscopic particles formed in the melt, neglecting the contribution of the gases, thus becomes the sum of contributions of $NaNO_2$ and Na_2CO_3. This is given by

$$\nu = (2x - 1)0.7 - 0.5x + 1 \qquad (6)$$

where the factor 0.7 accounts for solid–solution formation between $NaNO_2$ and $NaNO_3$. Substitution of $x = 0.84$ yields a value of $\nu = 1.06$. Allowing for the uncertainty of the ratio, *i.e.*, 0.68 ± 0.04, yields values of ν of 1.06 ± 0.01. This compares well with the limiting experimental values which range from 1.2 to 1.0. Thus the cryoscopic and voltammetric results are in agreement, and the reactions postulated in eq 4 and 5 are correct. This indicates that both reactions are occurring simultaneously in the melt. Further evidence is seen in Figure 3A, which shows that N_2O, while present, is much lower in intensity than CO_2. This would be expected from the low concentration of nitrite formed in the melt and the rapid reaction observed in this system.

It was noted earlier that the formation of NaOH was likely during reaction 4. The rapid disappearance of this species in the melt can be accounted for by

$$NaNO_3 + NaCOOH \longrightarrow NaNO_2 + NaOH + CO_2 \qquad (7)$$

which is immediately followed by

$$NaOH + {}^1/_2CO_2 \longrightarrow {}^1/_2Na_2CO_3 + {}^1/_2H_2O \qquad (8)$$

Note that the summation of reactions 7 and 8 is simply reaction 4.

$NaC_2H_3O_2$ in $NaNO_3$ and $NaNO_2$.—The results of the infrared analysis showed that the products of $NaC_2H_2O_2$ in $NaNO_3$ were Na_2CO_3, $NaNO_2$, CO_2, H_2O, and N_2O. In addition, an examination of the mass spectra of the gaseous products of this reaction gave mass numbers corresponding to H_2O and CO_2, as well as a gas of mass number 28. A gas of this mass number was not detected in the gaseous products from the formate reactions. The absence of any indication of CO in the infrared spectra has led to the assignment of the mass number of 28 to nitrogen. The products from the reaction of $NaC_2H_3O_2$ in $NaNO_2$ were found to be Na_2CO_3, H_2O, and N_2O. From stoichiometric considerations, it is felt that the reaction of acetate in nitrite constitutes the source of nitrogen in both this melt and $NaNO_3$. Finally, it is noteworthy that CO_2 was not formed in the nitrite melt.

These observations lead to the following reaction schemes

$$NaC_2H_3O_2 + 4NaNO_3 \longrightarrow 4NaNO_2 + {}^1/_2Na_2CO_3 + {}^3/_2CO_2 + {}^3/_2H_2O \qquad (9)$$

$$NaC_2H_3O_2 + 3NaNO_2 \longrightarrow 2Na_2CO_3 + {}^3/_2H_2O + {}^1/_2N_2O + N_2 \qquad (10)$$

---

[13] J. P. Frame, E. Rhodes, A. R. Ubbelohde, *Trans. Faraday Soc.*, **57**, 1075 (1961).

[14] E. M. Levin, C. R. Robbins, and H. F. McMurdie, "Phase Diagrams for Ceramists," The American Ceramic Society, Columbus, Ohio, 1964, p 338.

In general, these reactions were much slower than those involving NaCOOH. For example, the formate had completely reacted in less than 1 hr, while times ranging from 3 to 6 hr, depending on the amount of acetate, were required for the reaction to be completed at 325° in $NaNO_3$.

Using arguments similar to those advanced for the simpler formate–nitrate reactions, the moles of cryoscopic particles ν, formed per mole of acetate which reacted according to eq 9, becomes 3.3. As the amount of nitrite formed in the melt increases, the amount of cryoscopic particles approaches the limit given by the summation of eq 9 and 10, *i.e.*, $\nu \approx 1.6$. Again the contribution from the solubility of the gases has been neglected. Also, the times involved in obtaining a sufficient number of cooling curves at each concentration of acetate were well in excess of 6 hr, so that the reaction of acetate with nitrate is considered to be complete. The data in Figure 1 indicate a leveling off of the moles of particles generated in the melt at ν = 2.3–2.2. This value is obviously dependent on the rates of the reactions given in eq 9 and 10 and suggests that the contribution from the latter is significant. The cryoscopic results also suggest that the stoichiometry of both reactions is reasonable. That it is correct is shown when the voltammetric and chronopotentiometric results are taken into account.

The values of the ratio of moles of nitrite formed to moles of acetate added are in good agreement, *i.e.*, 2.3 ± 0.2 and 1.9 ± 0.2, respectively. The slower reaction rates observed in this system would tend to minimize the effect of diffusion and favor such a result. By using an analysis similar to that given for the formate reaction in nitrate, the ratio of nitrite formed to acetate added in reactions 9 and 10 is equal to $7x - 3$, where x represents the moles of acetate which reacted according to eq 9. Equating this to a mean value of the ratio of 2.1 ± 0.4 results in a value of $x = 0.73 \pm 0.06$ mol of acetate reacted. The total moles of cryoscopic particles formed from each mole of acetate is

$$\nu = (7x - 3)0.7 + 2(1 - x) + 0.5x \qquad (11)$$

Substitution of the values of x yields a ν of 2.4 ± 0.2, which is in excellent agreement with the cryoscopic results. Table IV summarizes the comparison of cryoscopic and electrochemical investigations.

Equation 10 predicts that 2 mol of carbonate will be formed from each mole of acetate which reacts in $NaNO_2$. Some recent work on the solvent properties of $NaNO_2$[15] showed that additions of $NaC_2H_3O_2$ did produce twice the expected number of particles in the melt. This can be taken as additional confirmation of the reaction given in eq 10 and the correctness of the over-all stoichiometry.

Some comments are necessary on the work of Shams El Din and El Hosary.[6] Their identification of carbonate and nitrite in the reaction of NaCOOH and $NaC_2H_3O_2$ in KNO_3 is essentially verified by this work. The reaction they proposed for formate reacting in KNO_3 postulates the presence of hydrogen as a product, *i.e.*

$$2NaCOOH + KNO_3 \longrightarrow Na_2CO_3 + KNO_2 + CO_2 + H_2 \qquad (12)$$

There was no evidence that hydrogen is produced in the all-sodium system. The reaction postulated for sodium acetate in KNO_3, *viz.*

$$4C_2H_3O_2^- + 5NO_3^- \longrightarrow 4CO_3^{2-} + NO_2^- + 4CH_3NO_2 \qquad (13)$$

does not correspond well to the reaction in the all-sodium systems. Thus the amount of cryoscopic particles predicted by eq 13 is too low if CH_3NO_2 is allowed to vaporize from the system and too high if CH_3NO_2 is assumed to dissolve in the melt. There was no spectroscopic evidence for the presence of CH_3NO_2, CH_4, or NO_2 in any of the systems examined in this work. Finally, the importance of the reaction of the carboxylic acid salt with the nitrite formed in the melt has not been taken into account. Nevertheless, it is true that the systems examined[6] did have mixed cations, *i.e.*, Na^+ and K^+, while this work has concentrated only on Na^+ systems. It is difficult to ascribe such tremendous differences in reaction schemes between the two melts as similar as sodium and potassium nitrate, and we must conclude that the reactions described in eq 4, 5, 9, and 10 are more representative of the behavior of carboxylic acid salts in molten nitrates.

The study of these systems was extended to include the cryoscopy of sodium propionate ($NaC_3H_5O_2$) in $NaNO_3$. The generation of particles as a function of propionate concentration is given in Figure 1. The initial values of ν are high, even taking into account the larger error in the first measurement. As the concentration of solute increases, the number of cryoscopic particles falls to 2.6–2.5 per mole added. Extrapolating from reactions 4 and 9, it appears as if three nitrate anions are required for each additional methyl group on the acid chain. Thus, a suggested scheme for propionate would be

$$NaC_3H_5O_2 + 7NaNO_3 \longrightarrow 7NaNO_2 + {}^1/_2Na_2CO_3 + {}^5/_2CO_2 + {}^5/_2H_2O \qquad (14)$$

Similar examination of eq 5 and 10 suggests that two nitrite anions are required for each additional methyl group on the acid chain. This produces

$$NaC_3H_5O_2 + 5NaNO_2 \longrightarrow 3Na_2CO_3 + {}^1/_2N_2O + {}^5/_2H_2O + 2N_2 \qquad (15)$$

where the only nongaseous product is Na_2CO_3, and CO_2 is not formed in the system. Equation 13, taken alone, predicts ν to be 5.3, while a sum of eq 13 and 14 provides a low value of $\nu = 2.4$. Agreement with experiment is reasonable and follows the pattern of the acetate–nitrate results.

In summary, it has been shown that NaCOOH and $NaC_2H_3O_2$ do react, even at temperatures near the melting point, in $NaNO_3$ and $NaNO_2$. The over-all reactions in nitrate melts generate nitrite and carbonate which remain in the solvent, while H_2O and CO_2, along with some N_2O and N_2, pass out of the solvent. In the nitrite melts, carbonate is produced in the melt, while N_2O, N_2, and H_2O pass out of the system. The

---

(15) T. R. Kozlowski and R. F. Bartholomew, *J. Electrochem. Soc.*, **114**, 937 (1967).

formation of nitrite as a reaction product in the nitrate melts results in a competition for additional carboxylic acid salt. The reactions with formate are more rapid than those with acetate, and caution is recommended in studying these systems.

Acknowledgment.—The efforts and assistance of Dennis A. Krygier in the cryoscopic and spectral phases of this work and the assistance of Stanley S. Lewek in obtaining the electrochemical data are greatly appreciated.

Contribution from Brookhaven National Laboratory,
Upton, New York 11973

The Reaction of Hydrogen with Alloys of Magnesium and Nickel and the Formation of Mg_2NiH_4[1]

By J. J. Reilly and R. H. Wiswall, Jr.

Received May 10, 1968

In the Mg–Ni system two intermetallic compounds are formed: Mg_2Ni and $MgNi_2$. $MgNi_2$ did not react with H_2 at pressures up to 400 psia and temperatures to 350°; however, Mg_2Ni reacted readily with H_2 at 300 psia and 325°. The product of the reaction was a new ternary hydride with the formula Mg_2NiH_4. The reaction was reversible and upon decomposition the original starting material was regenerated. The X-ray diffraction pattern of the product was indexed. Several pressure–composition isotherms were obtained. The dissociation pressure of the hydride was found to obey the relationship $\log P_{\text{atm}} = (-3360/T) + 6.389$ from which thermodynamic data were calculated. In the presence of excess Mg the pressure–composition isotherm exhibited two plateaus; the lower plateau is attributed to the formation of MgH_2 as evidenced by X-ray diffraction data and thermodynamic considerations. The presence of Mg_2Ni appeared to have a catalytic effect on the formation of MgH_2.

A previous article has described the reaction of hydrogen with magnesium–copper alloys.[2] In that article it was noted that the work was undertaken as part of an energy-storage program investigating the possibility of using reversible metal hydrides as a convenient and cheap means of storing hydrogen which is ultimately evolved and used as a fuel. This paper extends the discussion to the reaction of hydrogen with magnesium–nickel alloys at elevated temperatures and pressures. The system was found to be similar in some, but not all, respects to the Mg–Cu–H system.

Experimental Section

The materials used in this investigation were hydrogen gas obtained from the Matheson Co., Gold Label grade, having an assay of $>$99.99% H_2: zone-refined Mg rod, 0.25 in. in diameter and assaying 99.99% Mg with the major impurities being 20 ppm Fe and 20 ppm Zn; and nickel rod, 0.25 in. in diameter which assayed 99.99% Ni.

Although the procedure and apparatus were the same as that previously described in detail,[2] a brief summary may be helpful. The Mg–Ni alloys were prepared in an induction furnace under argon. The alloys were then transferred to a drybox, pulverized to -25 mesh, and introduced into a stainless steel high-pressure reactor. The reactor was removed from the drybox and attached to an experimental rack. The alloy samples were hydrided by exposing them to H_2 at $\sim$350 psia at temperatures up to 350°. The hydrided alloys could be decomposed by reducing the H_2 overpressure through the use of an evacuated gas reservoir or by outgassing under a dynamic vacuum.

Results and Discussion

Mg forms two intermetallic compounds with Ni, Mg_2Ni and $MgNi_2$.[3] Within the limits of the experimental conditions, *i.e.*, a maximum temperature of 350° and a maximum pressure of 400 psia, $MgNi_2$ did not react with H_2. However, Mg_2Ni reacted at a temperature of 325° at an H_2 pressure of 300 psia. Although initially the rate of reaction was somewhat slow, the kinetics improved markedly after several cycles of hydriding and decomposition, and after such pretreatment the alloys reacted readily at temperatures as low as 200° and an H_2 pressure as low as 200 psia.

In Figure 1 are shown three pressure–composition isotherms for the system Mg_2Ni–H_2. The initial composition of the sample was 45.9 wt % Mg and 54.6 wt % Ni; the theoretical composition of Mg_2Ni is 45.3 wt % Mg and 54.7 wt % Ni. The only phase initially present, as determined by an X-ray diffraction pattern of the sample, was Mg_2Ni. All of the isotherms ascend rapidly on the left indicating a narrow region where a solid solution of hydrogen in Mg_2Ni exists. This is followed by a wide plateau region, the initiation of which indicates the appearance of a new phase. To the right of the plateau each isotherm ascends very steeply. This portion of the isotherm is depicted as a dashed line because a small amount of solid hydride had to be decomposed before the first equilibrium point on the right could be defined and even a decomposition of a very small amount of material resulted in an equilibrium point on or near the plateau. The abrupt termination of the plateau indicates that the hydride formed has a definite stoichiometric composition. An X-ray diffraction pattern of the hydrided material showed no evidence of the presence of MgH_2, $MgNi_2$, Ni, or any

---

(1) This work was performed under the auspices of the U. S. Atomic Energy Commission.

(2) J. J. Reilly and R. H. Wiswall, *Inorg. Chem.*, **6**, 2220 (1967).

(3) J. Hansen, "Constitution of Binary Alloys," McGraw-Hill Book Co., Inc., New York, N. Y., 1958.